https://doi.org/10.1039/d0nr06198k

Electronic Supplementary Information
Optical Magnetic Lens: towards actively tunable terahertz optics

Georgii Shamuilov,[1,*] Katerina Domina, Vyacheslav Khardikov,[2,3]
Alexey Y. Nikitin,[4,5,6,†] and Vitaliy A. Goryashko[1,‡]

[1] *Department of Physics and Astronomy, Uppsala University, Lägerhyddsvägen 1, Uppsala, 75120, Sweden*
[2] *School of Radio Physics, V. N. Karazin Kharkiv National University, 4, Svobody Square, Kharkiv 61022, Ukraine*
[3] *Institute of Radio Astronomy of National Academy of Sciences of Ukraine, 4, Mystetstv Street,Kharkiv 61002, Ukraine*
[4] *Donostia International Physics Center (DIPC), 20018 Donostia-San Sebastián, Spain*
[5] *IKERBASQUE, Basque Foundation for Science, 48013 Bilbao, Spain*
[6] *CIC nanoGUNE BRTA, Tolosa Hiribidea 76, E-20018 Donostia-San Sebastián, Spain*

(Dated: December 17, 2020)

CONTENTS

(A) PERMITTIVITY TENSORS FOR VARIOUS MEDIA

For convenience of the reader, we include the expressions for elements of the dielectric permittivity tensor $\hat{\varepsilon}$ [eqn (1) in the article] for different materials considered in the paper.

(1) Plasmonic material

The simplest example is a thin film made of silver or gold, represented in the same way as magnetised plasma [1, 2]

$$\begin{aligned} 1+\varepsilon_\perp &= 1-\frac{\omega_p^2\,(\omega-i/\tau)}{\omega\left[(\omega-i/\tau)^2-\omega_c^2\right]},\\ \beta &= \frac{\omega_c\,\omega_p^2}{\omega\left[(\omega-i/\tau)^2-\omega_c^2\right]}. \end{aligned} \tag{1}$$

Here, ω is the frequency of light, ω_p is the material's plasma frequency and τ is the relaxation time. For silver, $\omega_p = 2321$ THz and $1/\tau = 5.513$ THz [3]. Assuming a quadratic magnetic field profile, as required for focusing, ω_c reads

$$\omega_c = \frac{qB_0}{m^* c}\left(1+\frac{r^2}{R_c^2}\right) = \omega_0 \mathcal{M}\left(1+\frac{r^2}{R_c^2}\right), \tag{2}$$

with $\mathcal{M} = m_e/m^* = 1$ for electrons in metal. Therefore, the focal length reads

$$f_\pm = \mp\frac{R_c^2}{d}\frac{\omega}{\omega_p^2\omega_0}\frac{[(\omega\mp\omega_0)^2+1/\tau^2]^2}{(\omega\mp\omega_0)^2-1/\tau^2} \approx \frac{\pm R_c^2}{d\tau^2\omega_p^2}\frac{\omega}{\omega_0}, \tag{3}$$

where the approximate value takes place under realistic magnetic fields [$\omega_0 = (2\pi)$ 28 GHz per 1 T of applied field], so that both ω and $\omega_0 \ll 1/\tau$; R_c is the curvature radius of the magnetic field and d is the film thickness.

(2) Ferrite

When working with non-magnetic materials, relative permeability $\mu = 1$, so that it is omitted and the eqn (2) of the article contains only the permittivity tensor $\hat{\varepsilon}$. For ferrites, the tensor form is traditionally assigned to $\hat{\mu}$, whereas ε has a scalar value ($\varepsilon = 15$ for YIG, Yttrium Iron Garnet). It is equivalent to write the paraxial wave equation (2) of the article as

$$\left(\Delta_\perp + 2ik\partial_z\right)\vec{E} = -k^2\left(\varepsilon\hat{\mu}-\hat{I}\right)\vec{E}, \tag{4}$$

where $\hat{\mu}$ has the same form as $\hat{\varepsilon}$ in eqn (1) in the article. Let us write down its elements ready for eqn (2) of the article [4]

$$\begin{aligned} 1+\varepsilon_\perp &= \varepsilon\left[1-\frac{\omega_M\,(\omega_c+i\alpha\omega)}{\omega^2-(\omega_c+i\alpha\omega)^2}\right],\\ \beta &= \frac{\varepsilon\;\omega\;\omega_M}{\omega^2-(\omega_c+i\alpha\omega)^2}. \end{aligned} \tag{5}$$

Here, $\omega_M = qM_s/m_e c$ with M_s being the saturation magnetisation ($\omega_M = 2\pi\cdot 49.8$ GHz for YIG), $\alpha = 2\cdot 10^{-4}$

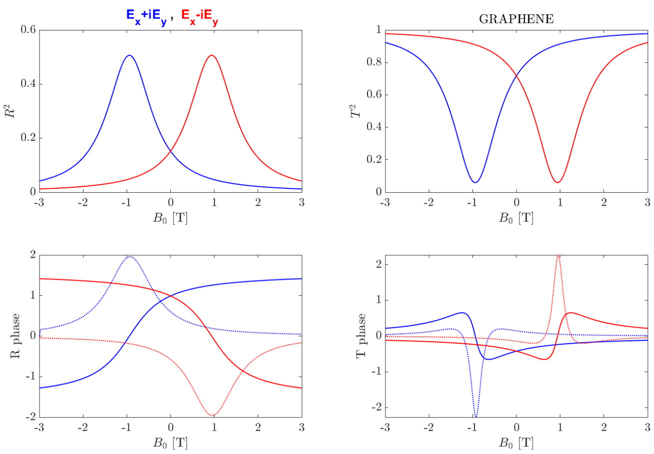

FIG. 1. Cyclotron resonance transition in graphene w.r.t. different circular polarisation components. In bottom panels, dotted curves are the derivatives of phases. Peak positive value of each is a working point for a lens.

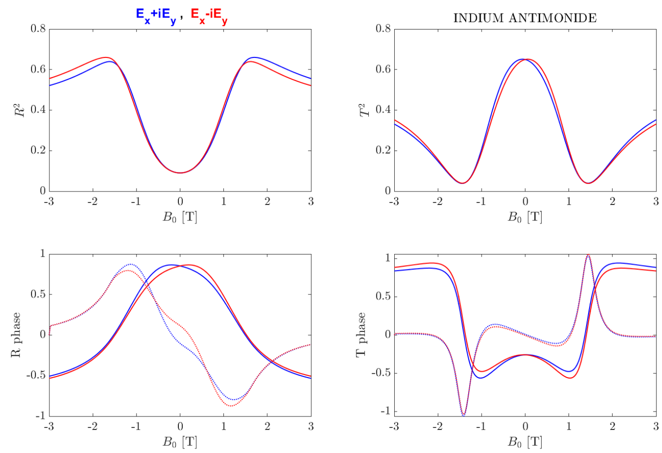

FIG. 2. Cyclotron resonance transition in InSb w.r.t. different circular polarisation components. In bottom panels, dotted curves are the derivatives of phases. Peak positive value of each is a working point for a lens.

(tangent loss angle, YIG) and ω_c is equivalent to Larmor frequency ω_L, because ferrimagnetism in YIG results from electronic spin, so that eqn (2) is applicable with $\mathcal{M} = 1$. In the proximity of the resonance, $\omega \approx \omega_0$, one may obtain expressions identical to eqn (8) and (9) of the main article, with $1/\tau = \alpha\omega_0$ and $\mathcal{A} = \omega_M\omega_0$.

(3) Graphene

Drude-like model for magnetised graphene is written in terms of conductivity as follows [5, 6]

$$\hat{\sigma} = \begin{pmatrix} \sigma_{xx} & -i\sigma_{xy} & 0 \\ i\sigma_{xy} & \sigma_{yy} & 0 \\ 0 & 0 & \sigma_{zz} \end{pmatrix},$$
$$\sigma_{xx} = \sigma_{yy} = \frac{q^2|\mu_c|}{\pi\hbar^2}\frac{i(\omega - i/\tau)}{(\omega - i/\tau)^2 - \omega_c^2}, \tag{6}$$
$$\sigma_{xy} = \frac{q^2|\mu_c|}{\pi\hbar^2}\frac{\omega_c}{(\omega - i/\tau)^2 - \omega_c^2}.$$

Here, μ_c is the chemical potential and $\hbar$ is the reduced Planck constant. Isotropic component σ_{zz} is of no further interest. Limiting to intraband transitions only, we follow the transformation $\hat{\varepsilon}_{\text{eff}} = (4\pi i/\omega d)\,\hat{\sigma}$ and find the elements of the effective permittivity tensor to read [compare to eqn (8) in the article]

$$1 + \varepsilon_\perp = \frac{-2\alpha_0|\mu_c|}{\pi\hbar}\,\frac{\lambda}{d}\,\frac{(\omega - i/\tau)}{(\omega - i/\tau)^2 - \omega_c^2},$$
$$\beta = \frac{2\alpha_0|\mu_c|}{\pi\hbar}\,\frac{\lambda}{d}\,\frac{\omega_c}{(\omega - i/\tau)^2 - \omega_c^2}. \tag{7}$$

Here α_0 is the fine structure constant and $\lambda = 2\pi c/\omega$ is the free-space wavelength, c is the speed of light. ω_c is given by eqn (2) with a variable $\mathcal{M} = m_e V_F^2/|\mu_c|$, V_F being the Fermi velocity. Upon series expansion, the focal length takes on the form of eqn (9) of the article. Corresponding constant is combined with thickness d and removes it from the expression for $f_\pm$, $\mathcal{A}d = 2\alpha_0|\mu_c|/\hbar = 1.95 \cdot 10^{19}$ [eV^{-1}s^{-2}]$\cdot|\mu_c|$ [eV]. An important feature of graphene-based OML is that only one polarisation component is focused resonantly, see Fig. 1. Thus, it allows for selective focusing of one polarisation or determining the polarisation content of incident light.

(4) Semiconductor

Magnetised semiconductors acquire the tensor form [eqn (1) in the article] of dielectric permittivity [7], with the elements identical to those given by eqn (8) of the article

$$1 + \varepsilon_\perp = \varepsilon_\infty - \frac{\varepsilon_\infty\omega_p^2\,(\omega - i/\tau)}{\omega\,[(\omega - i/\tau)^2 - \omega_c^2]},$$
$$\beta = \frac{\varepsilon_\infty\omega_c\,\omega_p^2}{\omega\,[(\omega - i/\tau)^2 - \omega_c^2]}. \tag{8}$$

For InSb, $\tau = 3.1$ ps, $\varepsilon_\infty = 15.68$, $\omega_p = 2.43$ THz, and $\mathcal{A} = \varepsilon_\infty\omega_p^2 = 9.26 \cdot 10^{25}$ s^{-2}. Upon series expansion, the focal length takes on the form of eqn (9) of the article. Unlike in graphene, $\mathcal{M}$ is a constant defined by the process used for manufacturing of the sample. In Table I (main article), $\mathcal{M} = 50$ is assumed. Similarly to ferrites, both polarisations are focused with different effective permittivities, see Fig. 2.

(5) Array of magnetic nanoparticles

From the eqn (9) in the article one can see that the focusing effect declines with the frequency increase. Yet it is still present at optical frequencies (near-infrared to visible). A periodic array of ferromagnetic nanoparticles (e.g. disks or pillars made of TbCo [8]) allows one to achieve a certain degree of focusing. Analytical calculations are very limited in this case, while numerical are demanding in computation power. We estimate the efficiency of such an array using a simplified full-wave numerical model. In the model, we sweep over the values of B_0 and determine the phase derivative $d\phi/dB_0$. In comparison with InSb (Fig. 2), it turns out to be a factor of 100 smaller, which is roughly the frequency ratio, $\omega_{\rm NIR} = (2\pi)$ 300 THz for 1 μm wavelength.

(6) Astrophysical plasma

In outer space there exist directed microwave sources such as cyclotron radiation in the magnetosphere of white dwarfs and pulsars [9, 10] or maser-like emission in the atmosphere of stars belonging to asymptotic giant branch [11]. Extremely high magnetic fields occur nearby pulsars and white dwarfs [9]. These fields are *non-uniform*. Hence, low density plasma nearby stellar objects with high magnetic fields may cause wavefront transformation and affect the perceived position of the source. Formulae given by eqn (1)-(3) are applicable, although with caution. Astrophysical plasma is often approximated as collisionless, $\tau \to \infty$. Alternatively, $1/\tau \ll \omega$ and ω_0. Thus, for quadratic magnetic fields

$$f_\pm \approx \mp \frac{R_c^2}{d\omega_p^2}\frac{\omega}{\omega_0}(\omega \mp \omega_0)^2, \tag{9}$$

which may be enough to make the source appear to be at a different distance. We would like to stress that *any* non-uniformity of the magnetic field over plasma gives a wavefront transformation. In most cases, it would act as aberrations and increase divergence of light.

(B) IMAGE FORMATION BY OPTICAL MAGNETIC LENS

To quantitatively characterise the focusing effect of the OML, we calculate the standard parameters of the focused optical beam: position of a new waist of the beam and the beam size at the waist. First, we compute how the beam size changes due to OML attenuation. The inhomogeneous attenuation coefficient $a_\pm = \log\big(|\mathcal{T}_\pm|\big)$ modifies the size of a new waist w as

$$\frac{1}{w^2} = \frac{1}{w_0^2} + \frac{|a''_\pm|}{2R_c^2}, \tag{10}$$

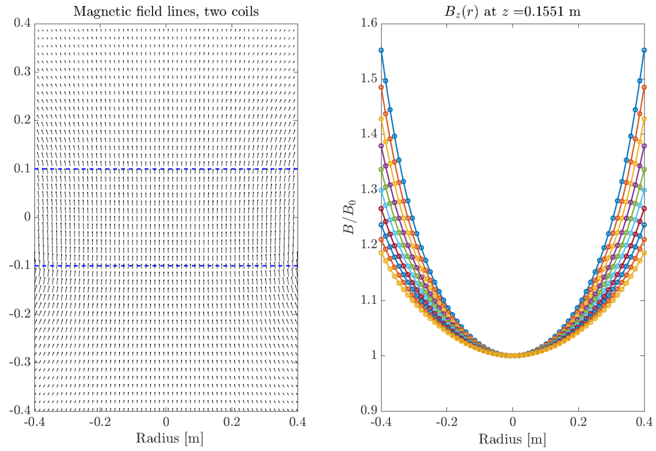

FIG. 3. **Left panel**: distribution of the magnetic field generated by two coils located at the dashed lines. **Right panel**: Transverse distributions of the magnetic field $B/B_0 = 1 + r^2/R_c^2$ given by different current ratios I_1/I_2 in the coils.

so that the beam size is reduced due to attenuation. Hence, the lens equation [12, 13] for Gaussian optical beams connecting the position of an object s and image s' (for real image $s' > 0$) is modified to read

$$\frac{1}{s + z_R^2/(s-f)} + \frac{w/w_0}{s'} = \frac{1}{f}, \tag{11}$$

where $z_R = \pi w_0^2/\lambda$ is the Rayleigh length. Eqn (11) shows that the image appears closer as compared to the case when the lens attenuation is zero and $w = w_0$. The beam size, w', at the new waist position s' is

$$w' = wf/\sqrt{(s-f)^2 + z_R^2} \tag{12}$$

and depends on the renormalised beam size w.

(C) FINE TUNING OF THE FOCAL LENGTH BY USING TWO COILS

Optical Magnetic Lens can be tuned precisely by controlling the current ratio of two coils, see Fig. 3. Importantly, the rate of retuning is limited only by the capabilities of power supplies that feed the coils. The plots in the figure were generated by direct integration of Biot-Savart law. In the center ($y = 0$ in the left panel), the field is most uniform, solenoid-like. Thus, an optimal point to locate the OML is slightly out of the coils, where transverse curvature of the magnetic field becomes profound. In the right-hand-side panel one may see that different values of I_1/I_2 provide different values of R_c.

(D) DERIVATION OF THE DIELECTRIC PERMITTIVITY TENSOR IN A NON-UNIFORM MAGNETIC FIELD

We derive the tensor of dielectric permittivity of plasma, $\hat{\varepsilon}$, in a non-uniform magnetic field $\vec{B}(r)$ from the first principles, namely: (i) *microscopic* Maxwell's equations for the electric and magnetic vectors $\vec{E}$ and $\vec{B}$; (ii) the Newton-Lorentz equation of motion of charge carriers in a thin layer; and (iii) the microscopic current in the form of the Klimontovich distribution. For simplicity, we consider the case of electrons in a plasma layer and a monochromatic wave.

Let us start with the motion of charge carriers in combined non-uniform fields (Cartesian coordinates)

$$\ddot{\vec{R}} = \frac{q}{m}\vec{E}(\vec{R})\mathrm{e}^{i\omega t} + \frac{q}{mc}\left[\dot{\vec{R}} \times \vec{B}(\vec{R})\right], \qquad (13)$$

where $\vec{R}(t)$ is the instantaneous position of the charge carrier, t is the time, $\vec{E}(\vec{R})$ is the electric field of an incident light wave of frequency ω, $\vec{B}(\vec{R})$ is the external static non-uniform magnetic field, c is the speed of light, q and m are the charge and mass of the particle respectively. In order to solve it, we expand it into series and thus split the motion into slow and fast components $\vec{R} = \vec{r} + \vec{\xi}$, $\vec{r}$ being a coordinate with a characteristic frequency reaching towards zero, while $\vec{\xi}$ oscillates with a frequency close to ω. We point out that only the fast component is radiative. The equation of motion for the fast component reads

$$\ddot{\vec{\xi}} = \frac{q}{m}\vec{E}(\vec{r})\mathrm{e}^{i\omega t} + \frac{q}{mc}\left[\dot{\vec{\xi}} \times \vec{B}(\vec{r})\right], \qquad (14)$$

where dependence of $\vec{r}$ on time can be neglected. With an ansatz $Y = \dot{\vec{\xi}}$, this equation reduces to a non-homogeneous system of differential equations of the first order $\dot{Y} - \hat{A}Y = F(t)$, where

$$\hat{A}(\vec{r}) = \begin{pmatrix} 0 & -\omega_c^z & \omega_c^y \\ \omega_c^z & 0 & -\omega_c^x \\ -\omega_c^y & \omega_c^x & 0 \end{pmatrix}, \quad F(\vec{r},t) = \frac{q}{m}\vec{E}(\vec{r})\mathrm{e}^{i\omega t} \qquad (15)$$

and $\vec{\omega}_c(\vec{r}) = q\vec{B}(\vec{r})/mc$. Finding a general solution by variation of parameters is straightforward, but tedious, so here we consider only one specific case when $\vec{B} = (0, 0, B_z)$ and $\omega_c = \omega_c^z$. Then, the solution for the fast component of acceleration of charge carriers reads

$$\dot{Y} = \ddot{\vec{\xi}} = \frac{q}{m}\mathrm{e}^{i\omega t}\begin{bmatrix} \frac{\omega^2 E_x(\vec{r}) + i\omega\omega_c(\vec{r})E_y(\vec{r})}{\omega^2 - \omega_c^2(\vec{r})} \\ \frac{\omega^2 E_y(\vec{r}) - i\omega\omega_c(\vec{r})E_x(\vec{r})}{\omega^2 - \omega_c^2(\vec{r})} \\ E_z(\vec{r}) \end{bmatrix}, \qquad (16)$$

where one can explicitly see the rise of polarisation mixing. Note that this radiative acceleration of charges contains dependence on the slow macroscopic coordinate $\vec{r}$.

Let us now turn to the slow component of motion manifested as particle drift. In non-uniform magnetic fields, charged particles experience slow drift along the axis transverse to both the field and the field gradient [14]. In non-uniform electric fields, such as the field of a Gaussian beam, particles are subject to ponderomotive drift from the region of strong field towards weaker field (away from the beam axis). Thus, the slow part of the equation of motion reads

$$\ddot{\vec{r}} = \frac{q}{m}(\vec{\xi}\cdot\vec{\nabla})\vec{E}(\vec{r})\mathrm{e}^{i\omega t} + \frac{q}{mc}\left[\dot{\vec{r}} \times \vec{B}(\vec{r}) + \dot{\vec{\xi}} \times (\vec{\xi}\cdot\vec{\nabla})\vec{B}(\vec{r})\right]. \qquad (17)$$

Here, $(\vec{\xi}\cdot\vec{\nabla})$ is a scalar differential operator sometimes called the directional derivative, $\vec{\nabla} = (\partial/\partial x, \partial/\partial y, \partial/\partial z)$ and $\vec{\xi} = \mathrm{e}^{i\omega t}(x_0, y_0, z_0)$ is a value of the fast coordinate that can be found by integrating eqn (16). To solve the eqn (17), one can time-average the terms that depend on $\vec{\xi}$. Again, a straightforward, but tedious process that we omit here. An example of such procedure applied to the electric field term can be found, for instance, in ref. [15].

Consider the non-uniform magnetic field given by $B_0 p(r)$ and a Gaussian incident beam $|\vec{E}| \sim \mathrm{e}^{-|r_\perp|^2/2w_0^2}$. From the time-averaged equation, it is possible to find the drift velocity. The interplay of electric and magnetic drift terms melts down to comparing the characteristic sizes of their profiles; namely, the beam waist size w_0 and the magnetic field curvature R_c. Both when $w_0 \gg R_c$ and $w_0 \approx R_c$, drift velocities have similar magnitude and opposite signs, which results in negligible net drift. If $w_0 \ll R_c$, the magnetic field-driven term dominates over the ponderomotive drift. However, the drift direction given by the axisymmetric magnetic field is tangential to the transverse coordinate $r_\perp$. Thus, non-uniformity of the field drives particles into slow spirals around the z-axis without critical effects on the concentration.

To check the consistency of this result, we solve the equations of motion [eqn (13)] numerically. The obtained numerical solution confirms the analytical result. In the dimensionless form, the equations depend on a ratio E_0/B_0. Greatly increasing this ratio does not change the qualitative behavior of the system, but increases the area occupied by it (a possible limit by the size of the sample).

Having established the absence of charge density disturbance, we finally assume a hydrodynamic current in the form of Klimontovich distribution

$$\vec{j} = qn\vec{v} = qn\dot{\vec{\xi}}. \qquad (18)$$

From microscopic Maxwell's equations, electromagnetic wave equation follows, with the source term given by the current in eqn (18)

$$\left(\Delta - \frac{1}{c^2}\frac{\partial^2}{\partial t^2}\right)\vec{E}(\vec{r},t) = \frac{4\pi}{c^2}\dot{\vec{j}} = \frac{4\pi qn}{c^2}\ddot{\vec{\xi}}. \qquad (19)$$

Using the eqn (16), we obtain

$$\left(\Delta + \frac{\omega^2}{c^2}\right)\begin{bmatrix} E_x(\vec{r}) \\ E_y(\vec{r}) \\ E_z(\vec{r}) \end{bmatrix} = \frac{\omega_p^2}{c^2}\begin{bmatrix} \frac{\omega^2 E_x(\vec{r}) + i\omega\omega_c(\vec{r})E_y(\vec{r})}{\omega^2-\omega_c^2(\vec{r})} \\ \frac{\omega^2 E_y(\vec{r}) - i\omega\omega_c(\vec{r})E_x(\vec{r})}{\omega^2-\omega_c^2(\vec{r})} \\ E_z(\vec{r}) \end{bmatrix}, \tag{20}$$

where $\omega_p = \sqrt{4\pi q^2 n/m}$ is the plasma frequency. The right-hand-side of this equation (source term) can be easily included on the left as a dielectric permittivity ε. The presence of imaginary cross-terms there indicates that it has a tensor form. Upon equating corresponding matrix products, one can find the permittivity tensor to read

$$\hat{\varepsilon} = \begin{pmatrix} 1+\varepsilon_\perp & -i\beta & 0 \\ i\beta & 1+\varepsilon_\perp & 0 \\ 0 & 0 & \varepsilon_\parallel \end{pmatrix}, \quad \varepsilon_\perp = \frac{-\omega_p^2(\omega - i/\tau)}{\omega\left[(\omega-i/\tau)^2 - \omega_c^2(\vec{r})\right]}$$
$$\varepsilon_\parallel = 1 - \frac{\omega_p^2}{\omega(\omega-i/\tau)}, \quad \beta = \frac{\omega_p^2\omega_c(\vec{r})}{\omega\left[(\omega-i/\tau)^2-\omega_c^2(\vec{r})\right]}. \tag{21}$$

Here, we included the phenomenological absorption represented by the relaxation time τ. Thus, we have shown that under non-uniform magnetic fields the dielectric permittivity tensor for optical beams retains its form while acquiring a coordinate dependence given by the applied field.

* e-mail: georgii.shamuilov@physics.uu.se
† e-mail: alexey@dipc.org
‡ corresponding author: vitaliy.goryashko@physics.uu.se

[1] V. Nikolskiy and T. Nikolskaya, *Electrodynamics and radio wave propagation* (Nauka Publ., 1989) p. 508.
[2] J. Bergman, Physics of Plasmas **7**, 3476 (2000).
[3] M. G. Blaber, M. D. Arnold, and M. J. Ford, The Journal of Physical Chemistry C **113**, 3041 (2009).
[4] D. Pozar, *Microwave Engineering, 4th Edition* (Wiley, 2011) Chap. 9.
[5] M. Tymchenko, A. Y. Nikitin, and L. Martín-Moreno, ACS Nano **7**, 9780 (2013).
[6] A. Ferreira, J. Viana-Gomes, Y. V. Bludov, V. Pereira, N. M. R. Peres, and A. H. C. Neto, Physical Review B **84**, 235410 (2011).
[7] A. A. P. Gibson, L. E. Davis, and S. I. Sheikh, Electromagnetics **15**, 615 (1995).
[8] A. Ciuciulkaite, K. Mishra, M. V. Moro, I.-A. Chioar, R. M. Rowan-Robinson, S. Parchenko, A. Kleibert, B. Lindgren, G. Andersson, C. S. Davies, A. Kimel, M. Berritta, P. M. Oppeneer, A. Kirilyuk, and V. Kapaklis, Physical Review Materials **4**, 104418 (2020).
[9] V. Zheleznyakov, *Radiation in Astrophysical Plasmas*, Astrophysics and Space Science Library (Springer Netherlands, 2012) Chap. 1.
[10] R. A. Treumann, The Astronomy and Astrophysics Review **13**, 229 (2006).
[11] W. H. T. Vlemmings, P. Diamond, and H. van Langevelde, in *Mass-Losing Pulsating Stars and their Circumstellar Matter* (Springer Netherlands, 2003) pp. 291–294.
[12] S. A. Self, Applied optics **22**, 658 (1983).
[13] B. E. Saleh and M. C. Teich, *Fundamentals of photonics* (John Wiley & Sons, 2019).
[14] J. Jackson, *Classical electrodynamics* (Wiley, 2007).
[15] S. Usikov, *Nonlinear Physics*, Contemporary concepts in physics (Taylor & Francis, 1988) Chap. 2.